



HAL
open science

Search for Supersymmetric Particles with R-Parity Violating Decays in e^+e^- Collisions at \sqrt{s} up to 209GeV

A. Heister, S. Schael, R. Barate, R. Bruneliere, I. de Bonis, D. Decamp, C. Goy, S. Jezequel, J P. Lees, F. Martin, et al.

► **To cite this version:**

A. Heister, S. Schael, R. Barate, R. Bruneliere, I. de Bonis, et al.. Search for Supersymmetric Particles with R-Parity Violating Decays in e^+e^- Collisions at \sqrt{s} up to 209GeV. European Physical Journal C: Particles and Fields, 2003, 31, pp.1-16. in2p3-00019981

HAL Id: in2p3-00019981

<https://hal.in2p3.fr/in2p3-00019981>

Submitted on 13 Nov 2003

HAL is a multi-disciplinary open access archive for the deposit and dissemination of scientific research documents, whether they are published or not. The documents may come from teaching and research institutions in France or abroad, or from public or private research centers.

L'archive ouverte pluridisciplinaire **HAL**, est destinée au dépôt et à la diffusion de documents scientifiques de niveau recherche, publiés ou non, émanant des établissements d'enseignement et de recherche français ou étrangers, des laboratoires publics ou privés.

Search for Supersymmetric Particles
with R-Parity Violating Decays
in e^+e^- Collisions at \sqrt{s} up to 209 GeV

The ALEPH Collaboration*)

Abstract

Searches for the pair production of supersymmetric particles under the assumption that R-parity is violated via a single dominant $LL\bar{E}$, $LQ\bar{D}$ or $\bar{U}\bar{D}\bar{D}$ coupling are performed using the data collected by the ALEPH detector at LEP at centre-of-mass energies from 189 to 209 GeV. The numbers of observed candidate events in the data are in agreement with the Standard Model expectation, and limits on the production cross sections and on the masses of charginos, sleptons, squarks and sneutrinos are derived.

(Submitted to the European Physical Journal C)

*) See next pages for the list of authors

The ALEPH Collaboration

A. Heister, S. Schael

Physikalisches Institut der RWTH-Aachen, D-52056 Aachen, Germany

R. Barate, R. Brunelière, I. De Bonis, D. Decamp, C. Goy, S. Jezequel, J.-P. Lees, F. Martin, E. Merle, M.-N. Minard, B. Pietrzyk, B. Trocmé

Laboratoire de Physique des Particules (LAPP), IN²P³-CNRS, F-74019 Annecy-le-Vieux Cedex, France

S. Bravo, M.P. Casado, M. Chmeissani, J.M. Crespo, E. Fernandez, M. Fernandez-Bosman, Ll. Garrido,¹⁵ M. Martinez, A. Pacheco, H. Ruiz

Institut de Física d'Altes Energies, Universitat Autònoma de Barcelona, E-08193 Bellaterra (Barcelona), Spain⁷

A. Colaleo, D. Creanza, N. De Filippis, M. de Palma, G. Iaselli, G. Maggi, M. Maggi, S. Nuzzo, A. Ranieri, G. Raso,²⁴ F. Ruggieri, G. Selvaggi, L. Silvestris, P. Tempesta, A. Tricomi,³ G. Zito

Dipartimento di Fisica, INFN Sezione di Bari, I-70126 Bari, Italy

X. Huang, J. Lin, Q. Ouyang, T. Wang, Y. Xie, R. Xu, S. Xue, J. Zhang, L. Zhang, W. Zhao

Institute of High Energy Physics, Academia Sinica, Beijing, The People's Republic of China⁸

D. Abbaneo, P. Azzurri, T. Barklow,²⁶ O. Buchmüller,²⁶ M. Cattaneo, F. Cerutti, B. Clerbaux,²³ H. Drevermann, R.W. Forty, M. Frank, F. Gianotti, J.B. Hansen, J. Harvey, D.E. Hutchcroft, P. Janot, B. Jost, M. Kado,² P. Mato, A. Moutoussi, F. Ranjard, L. Rolandi, D. Schlatter, G. Sguazzoni, W. Tejessy, F. Teubert, A. Valassi, I. Videau, J.J. Ward

European Laboratory for Particle Physics (CERN), CH-1211 Geneva 23, Switzerland

F. Badaud, S. Dessagne, A. Falvard,²⁰ D. Fayolle, P. Gay, J. Jousset, B. Michel, S. Monteil, D. Pallin, J.M. Pascolo, P. Perret

Laboratoire de Physique Corpusculaire, Université Blaise Pascal, IN²P³-CNRS, Clermont-Ferrand, F-63177 Aubière, France

J.D. Hansen, J.R. Hansen, P.H. Hansen, B.S. Nilsson

Niels Bohr Institute, 2100 Copenhagen, DK-Denmark⁹

A. Kyriakis, C. Markou, E. Simopoulou, A. Vayaki, K. Zachariadou

Nuclear Research Center Demokritos (NRCD), GR-15310 Attiki, Greece

A. Blondel,¹² J.-C. Brient, F. Machefert, A. Rougé, M. Swynghedauw, R. Tanaka, H. Videau

Laboratoire Leprince-Ringuet, Ecole Polytechnique, IN²P³-CNRS, F-91128 Palaiseau Cedex, France

V. Ciulli, E. Focardi, G. Parrini

Dipartimento di Fisica, Università di Firenze, INFN Sezione di Firenze, I-50125 Firenze, Italy

A. Antonelli, M. Antonelli, G. Bencivenni, F. Bossi, G. Capon, V. Chiarella, P. Laurelli, G. Mannocchi,⁵ G.P. Murtas, L. Passalacqua

Laboratori Nazionali dell'INFN (LNF-INFN), I-00044 Frascati, Italy

J. Kennedy, J.G. Lynch, P. Negus, V. O'Shea, A.S. Thompson

Department of Physics and Astronomy, University of Glasgow, Glasgow G12 8QQ, United Kingdom¹⁰

S. Wasserbaech

Department of Physics, Haverford College, Haverford, PA 19041-1392, U.S.A.

R. Cavanaugh,⁴ S. Dhamotharan,²¹ C. Geweniger, P. Hanke, V. Hepp, E.E. Kluge, G. Leibenguth, A. Putzer, H. Stenzel, K. Tittel, M. Wunsch¹⁹

Kirchhoff-Institut für Physik, Universität Heidelberg, D-69120 Heidelberg, Germany¹⁶

R. Beuselinck, W. Cameron, G. Davies, P.J. Dornan, M. Girone,¹ R.D. Hill, N. Marinelli, J. Nowell, S.A. Rutherford, J.K. Sedgbeer, J.C. Thompson,¹⁴ R. White

Department of Physics, Imperial College, London SW7 2BZ, United Kingdom¹⁰

V.M. Ghete, P. Girtler, E. Kneringer, D. Kuhn, G. Rudolph

Institut für Experimentalphysik, Universität Innsbruck, A-6020 Innsbruck, Austria¹⁸

E. Bouhova-Thacker, C.K. Bowdery, D.P. Clarke, G. Ellis, A.J. Finch, F. Foster, G. Hughes, R.W.L. Jones, M.R. Pearson, N.A. Robertson, M. Smizanska

Department of Physics, University of Lancaster, Lancaster LA1 4YB, United Kingdom¹⁰

O. van der Aa, C. Delaere, V. Lemaitre

Institut de Physique Nucléaire, Département de Physique, Université Catholique de Louvain, 1348 Louvain-la-Neuve, Belgium

U. Blumenschein, F. Hölldorfer, K. Jakobs, F. Kayser, K. Kleinknecht, A.-S. Müller, B. Renk, H.-G. Sander, S. Schmeling, H. Wachsmuth, C. Zeitnitz, T. Ziegler

Institut für Physik, Universität Mainz, D-55099 Mainz, Germany¹⁶

A. Bonissent, P. Coyle, C. Curtil, A. Ealet, D. Fouchez, P. Payre, A. Tilquin

Centre de Physique des Particules de Marseille, Univ Méditerranée, IN²P³-CNRS, F-13288 Marseille, France

F. Ragusa

Dipartimento di Fisica, Università di Milano e INFN Sezione di Milano, I-20133 Milano, Italy.

A. David, H. Dietl, G. Ganis,²⁷ K. Hüttmann, G. Lütjens, W. Männer, H.-G. Moser, R. Settles, G. Wolf
Max-Planck-Institut für Physik, Werner-Heisenberg-Institut, D-80805 München, Germany¹⁶

J. Boucrot, O. Callot, M. Davier, L. Duflot, J.-F. Grivaz, Ph. Heusse, A. Jacholkowska,⁶ L. Serin, J.-J. Veillet, C. Yuan

Laboratoire de l'Accélérateur Linéaire, Université de Paris-Sud, IN²P³-CNRS, F-91898 Orsay Cedex, France

G. Bagliesi, T. Boccali, L. Foà, A. Giammanco, A. Giassi, F. Ligabue, A. Messineo, F. Palla, G. Sanguinetti, A. Sciabà, R. Tenchini,¹ A. Venturi,¹ P.G. Verdini

Dipartimento di Fisica dell'Università, INFN Sezione di Pisa, e Scuola Normale Superiore, I-56010 Pisa, Italy

O. Awunor, G.A. Blair, G. Cowan, A. Garcia-Bellido, M.G. Green, L.T. Jones, T. Medcalf, A. Misiejuk, J.A. Strong, P. Teixeira-Dias

Department of Physics, Royal Holloway & Bedford New College, University of London, Egham, Surrey TW20 OEX, United Kingdom¹⁰

R.W. Clift, T.R. Edgecock, P.R. Norton, I.R. Tomalin

Particle Physics Dept., Rutherford Appleton Laboratory, Chilton, Didcot, Oxon OX11 0QX, United Kingdom¹⁰

B. Bloch-Devaux, D. Boumediene, P. Colas, B. Fabbro, E. Lançon, M.-C. Lemaire, E. Locci, P. Perez, J. Rander, B. Tuchming, B. Vallage

CEA, DAPNIA/Service de Physique des Particules, CE-Saclay, F-91191 Gif-sur-Yvette Cedex, France¹⁷

N. Konstantinidis, A.M. Litke, G. Taylor

Institute for Particle Physics, University of California at Santa Cruz, Santa Cruz, CA 95064, USA²²

C.N. Booth, S. Cartwright, F. Combley,²⁵ P.N. Hodgson, M. Lehto, L.F. Thompson
*Department of Physics, University of Sheffield, Sheffield S3 7RH, United Kingdom*¹⁰

A. Böhrer, S. Brandt, C. Grupen, J. Hess, A. Ngac, G. Prange
*Fachbereich Physik, Universität Siegen, D-57068 Siegen, Germany*¹⁶

C. Borean, G. Giannini
Dipartimento di Fisica, Università di Trieste e INFN Sezione di Trieste, I-34127 Trieste, Italy

H. He, J. Putz, J. Rothberg
Experimental Elementary Particle Physics, University of Washington, Seattle, WA 98195 U.S.A.

S.R. Armstrong, K. Berkelman, K. Cranmer, D.P.S. Ferguson, Y. Gao,¹³ S. González, O.J. Hayes, H. Hu, S. Jin, J. Kile, P.A. McNamara III, J. Nielsen, Y.B. Pan, J.H. von Wimmersperg-Toeller, W. Wiedenmann, J. Wu, Sau Lan Wu, X. Wu, G. Zobernig
*Department of Physics, University of Wisconsin, Madison, WI 53706, USA*¹¹

G. Dissertori
Institute for Particle Physics, ETH Höggerberg, 8093 Zürich, Switzerland.

¹Also at CERN, 1211 Geneva 23, Switzerland.

²Now at Fermilab, PO Box 500, MS 352, Batavia, IL 60510, USA

³Also at Dipartimento di Fisica di Catania and INFN Sezione di Catania, 95129 Catania, Italy.

⁴Now at University of Florida, Department of Physics, Gainesville, Florida 32611-8440, USA

⁵Also Istituto di Cosmo-Geofisica del C.N.R., Torino, Italy.

⁶Also at Groupe d'Astroparticules de Montpellier, Université de Montpellier II, 34095, Montpellier, France.

⁷Supported by CICYT, Spain.

⁸Supported by the National Science Foundation of China.

⁹Supported by the Danish Natural Science Research Council.

¹⁰Supported by the UK Particle Physics and Astronomy Research Council.

¹¹Supported by the US Department of Energy, grant DE-FG0295-ER40896.

¹²Now at Departement de Physique Corpusculaire, Université de Genève, 1211 Genève 4, Switzerland.

¹³Also at Department of Physics, Tsinghua University, Beijing, The People's Republic of China.

¹⁴Supported by the Leverhulme Trust.

¹⁵Permanent address: Universitat de Barcelona, 08208 Barcelona, Spain.

¹⁶Supported by Bundesministerium für Bildung und Forschung, Germany.

¹⁷Supported by the Direction des Sciences de la Matière, C.E.A.

¹⁸Supported by the Austrian Ministry for Science and Transport.

¹⁹Now at SAP AG, 69185 Walldorf, Germany

²⁰Now at Groupe d'Astroparticules de Montpellier, Université de Montpellier II, 34095 Montpellier, France.

²¹Now at BNP Paribas, 60325 Frankfurt am Mainz, Germany

²²Supported by the US Department of Energy, grant DE-FG03-92ER40689.

²³Now at Institut Inter-universitaire des hautes Energies (IIHE), CP 230, Université Libre de Bruxelles, 1050 Bruxelles, Belgique

²⁴Also at Dipartimento di Fisica e Tecnologia Relative, Università di Palermo, Palermo, Italy.

²⁵Deceased.

²⁶Now at SLAC, Stanford, CA 94309, U.S.A

²⁷Now at INFN Sezione di Roma II, Dipartimento di Fisica, Università di Roma Tor Vergata, 00133 Roma, Italy.

1 Introduction

The search for supersymmetric particles addressed in this paper is performed in the framework of the minimal supersymmetric extension of the Standard Model (MSSM) [1] with R-parity violation. Conservation of R-parity [2] is usually assumed in order to prevent experimentally forbidden low energy processes (e.g. fast proton decay). Nevertheless this symmetry is not required theoretically, and models with R-parity violation can be constructed, which are compatible with experimental constraints.

A generic model can be built from the R-parity violating terms of the superpotential [3]

$$W_{\mathbb{R}_p} = \lambda_{ijk} L_i L_j \bar{E}_k + \lambda'_{ijk} L_i Q_j \bar{D}_k + \lambda''_{ijk} \bar{U}_i \bar{D}_j \bar{D}_k, \quad (1)$$

where \bar{D}, \bar{U} and \bar{E} are down-like quark, up-like quark and lepton singlet superfields, Q and L are the quark and lepton doublet superfields; λ, λ' and λ'' are Yukawa couplings and $i, j, k = 1, 2, 3$ are generation indices. The presence of such R-parity violating terms implies that the lightest supersymmetric particle (LSP) is unstable and that supersymmetric particles can decay directly to Standard Model particles.

The sparticle decays which proceed directly to Standard Model particles are called *direct* decays (Fig. 1). Decays in which the sparticle first decays, conserving R-parity, to the lightest neutralino are referred to as *indirect* decays (Fig. 2). Other cascade decays are possible but not considered in the following.

The following assumptions are made throughout:

- All three terms in Equation (1) are addressed, however only one term at a time is considered to be nonzero for a specific set of indices (i, j and k). Unless otherwise stated the derived limits correspond to the choice of indices for the coupling giving the least stringent limit.
- The lifetime of the sparticles can be neglected, i.e. the mean flight path is less than 1 cm. This assumption restricts the sensitivity of the search to R-parity violating couplings greater than 10^{-4} for gauginos and 10^{-7} for direct decays of sfermions, and constrains the mass of the neutralino to be above 10 GeV/ c^2 [4].
- Results are interpreted within the framework of the MSSM with R-parity violation. In addition to R-parity violating couplings, the parameters are the gaugino mass terms (M_i), the sfermion masses ($m_{\tilde{f}}$), the ratio of the Higgs doublet vacuum expectation values ($\tan\beta$), the higgsino mass term (μ) and the trilinear couplings (A_i). Gaugino mass term unification at the GUT scale is assumed, giving the condition $M_1 = \frac{5}{3}M_2 \tan^2 \theta_W$ at the electroweak scale.
- For chargino and neutralino decays, only large values of sfermion masses are considered, with the consequence that the *direct* decays of the lightest chargino and the next-to-lightest neutralino are suppressed. It also implies three-body kinematics for the lightest neutralino decay.

The searches presented in this paper cover all types of sparticle pair production; the case of single sneutrino production is addressed in [5]. The results reported are based on all data collected by the ALEPH detector in the years 1998, 1999 and 2000. The new data collected in year 2000 at centre-of-mass energies up to 209 GeV is grouped in two samples of 81.6 pb^{-1} and 133.7 pb^{-1} luminosity at $\langle\sqrt{s}\rangle = 204.9 \text{ GeV}$ and 206.5 GeV , respectively. Those two samples will be called 205 GeV and 207 GeV in the following.

This paper is organized as follows: after a brief description of the ALEPH detector, the Monte Carlo generators used for signal and background are listed in Section 2. The selections used for all topologies and the results obtained when those selections are applied on data and Monte Carlo events are presented in Section 3. Section 4 gives the interpretations, within the MSSM framework, of the absence of any supersymmetric signal in the data. A summary of the results is presented in Section 5.

2 The ALEPH Detector and Monte Carlo generators

The ALEPH detector is described in detail in Ref. [6]. An account of the performance of the detector and a description of the standard analysis algorithms can be found in Ref. [7]. Here, only a brief description of the detector components and the algorithms relevant for this analysis is given.

The trajectories of charged particles are measured with a silicon vertex detector, a cylindrical drift chamber, and a large time projection chamber (TPC). The central detectors are immersed in a 1.5 T axial magnetic field provided by a superconducting solenoidal coil. The electromagnetic calorimeter (ECAL), placed between the TPC and the coil, is a highly segmented sampling calorimeter which is used to identify electrons and photons and to measure their energies. The hadron calorimeter (HCAL) consists of the iron return yoke of the magnet instrumented with streamer tubes. It provides a measurement of hadronic energy and, together with the external muon chambers, muon identification. The luminosity monitors extend the calorimetric coverage down to 34 mrad from the beam axis. The calorimetric and tracking information are combined in an energy flow algorithm which gives a measure of the total energy with an uncertainty of $(0.6\sqrt{E} + 0.6) \text{ GeV}$.

Electron identification is primarily based upon the matching between the measured momentum of the charged track and the energy deposited in the ECAL. Additional information from the shower profile in the ECAL and the measured rate of specific ionisation energy loss in the TPC are also used. Muons are separated from hadrons by their characteristic pattern in HCAL and the presence of associated hits in the muon chambers.

The signal topologies were simulated using the SUSYGEN Monte Carlo program [8], modified as described in Ref. [9]. The events were subsequently passed either through a full simulation, or through a faster simplified simulation of the ALEPH detector for interpolation purposes.

Samples of all major backgrounds were generated and passed through the full simulation. The PYTHIA generator [10] was used to produce $q\bar{q}$ events and four-fermion final states from $W\nu$, ZZ and Zee . Pairs of W bosons were generated with KORALW [11]. Pair production of leptons was simulated with BHWIDE [12] (electrons) and KORALZ [13] (muons and taus). The $\gamma\gamma \rightarrow f\bar{f}$ processes were generated with PHOT02 [14].

3 Selections and results

The selections were optimized to give the minimum expected 95% C.L. excluded cross section in the absence of a signal for masses close to the high end of the expected sensitivity. Selection efficiencies were determined as a function of the SUSY particle masses and the generation structure of the R-parity violating couplings λ_{ijk} , λ'_{ijk} and λ''_{ijk} . Two new selections have been added with respect to previous publications, the others are unchanged from those used in Refs. [4, 9, 15, 16, 17], except for centre-of-mass energy rescaling. The new selections : “Many jets + Taus” and “Four jets + Taus” address topologies with many jets and taus and are used in the search for indirect stau decays. The set of cuts is shown in Table 1. Tau production is tagged by missing energy and a low multiplicity jet. The corresponding event variable (N_{jet-ch}^{min}) is the number of charged tracks in the lowest multiplicity jet when forcing the event into four jets.

Table 1: The list of cuts for the “Four Jets + Taus” and “Many Jets + Taus” selections, as used for the search for indirect stau decays via a $\bar{U}\bar{D}\bar{D}$ operator. N_{jet-ch}^{min} is the number of charged tracks in the lowest multiplicity jet. The other variables are defined in Ref. [9]

Four Jets + Taus	Many Jets + Taus
$N_{ch} > 8$ $ p_z^{miss} /p^{miss} < 0.95$, $0.5 < E_{vis}/\sqrt{s} < 0.95$ $E_{jet}^{em} < 95\%E_{jet}$, $E_T > 45$ GeV $N_{jet-ch}^{min} < 5$	
$0.6 < T < 0.92$ $y_4 > 0.005$	$0.6 < T < 0.97$ $y_4 > 0.005$ $y_6 > 0.0025$
$ M_{12-34} < 10$ GeV/ c^2 $ M_{12+34} - 2M_{\tilde{\tau}} < 5$ GeV/ c^2	

3.1 Selections for a dominant $LL\bar{E}$ coupling

Direct decays with a dominant $LL\bar{E}$ coupling only involve leptons and neutrinos in the final states. When indirect decays occur, additional leptons, neutrinos and jets are produced.

Table 2: The observed numbers of events in the year 2000 data sample and the corresponding background expectations for the $LL\bar{E}$ selections. The selections are given together with the references to the papers in which they are described.

Selection	Ref.	205 GeV		207 GeV	
		Data	Background	Data	Background
Leptons and Hadrons	[4, 15]	5	3.5	8	5.6
6 Leptons + \cancel{E}	[4]	0	0.5	0	0.8
4 Leptons + \cancel{E}	[4]	1	2.3	4	3.1
$llll$	[4]	1	3.8	3	3.5
$ll\tau\tau$	[4]	0	1.1	1	1.4
$\tau\tau\tau\tau$	[4]	1	2.4	5	2.6
Acoplanar Leptons	[4, 9]	71	89	139	138

The decay topologies consist either of purely leptonic final states — as few as two acoplanar leptons in the simplest case (direct slepton decay) or as many as six leptons plus four neutrinos in the most complicated case (indirect chargino decay) — or of multi-jet and multi-lepton final states.

The various selections addressing the above topologies are summarized in Table 2 together with the references of the papers in which detailed descriptions of the selection cuts can be found. The numbers of selected data candidates and the expected backgrounds are also given in this table.

3.2 Selections for a dominant $LQ\bar{D}$ Coupling

For a dominant $LQ\bar{D}$ operator the event topologies are mainly characterized by large hadronic activity, possibly with some leptons and some missing energy. In the simplest case the topology consists of four jets, and in the more complicated scenarios, of several jets or leptons, with or without missing mass. The various selections are listed in Table 3 together with the corresponding numbers of observed data candidates and expected background events.

3.3 Selections for a dominant $\bar{U}\bar{D}\bar{D}$ coupling

For a dominant $\bar{U}\bar{D}\bar{D}$ operator the final states are characterized by topologies having many hadronic jets, possibly associated with leptons or taus and missing energy.

These selections rely mainly on two characteristics of the signal events: the reconstructed mass of pair produced sparticles and the presence of many jets in the final state. In Table 4

the list of all the selections is given, together with the numbers of data candidates and expected background events.

Table 3: The observed numbers of events in the year 2000 data sample and the corresponding background expectations for the $LQ\bar{D}$ selections. The selections are given together with the references to the papers in which they are described.

Selection	Ref.	205 GeV		207 GeV	
		Data	Background	Data	Background
MultiJets + Leptons	[15, 16]	5	5.2	14	8.6
Jets-HM	[15]	3	2.2	7	3.3
4 Jets + 2τ	[15, 16]	9	5.0	6	8.0
Four-Jets	[15, 16]	341	348	541	561
2 Jets + 2τ	[15, 16]	7	4.9	7	7.9
AJ-H	[17]	12	10.7	19	18.5
4JH	[17]	4	3.7	4	5.9
5 Jets + 1 Iso. ℓ	[15]	1	2.1	2	3.7
4 Jets + 2 Iso. ℓ	[15]	0	1.3	1	2.0

Table 4: The observed numbers of events in the year 2000 data sample and the corresponding background expectations for the $\bar{U}\bar{D}\bar{D}$ selections. The selections are given together with the references to the papers in which they are described.

Selection	Ref.	205 GeV		207 GeV	
		Data	Background	Data	Background
Four Jets Broad	[9]	53	51.8	72	84.1
Many Jets	[9]	6	3.8	6	6.2
Many Jets + Leptons	[9]	6	7.6	14	12
Four Jets + 2 Leptons	[9]	2	2.1	4	3.6
Many Jets + 2 Leptons	[9]	3	2.9	1	4.9
Four Jets+ \cancel{E}	[9, 15]	32	33.3	48	51.4
Many Jets+ \cancel{E}	[9, 15]	30	33.3	48	51.4
Four Jets + Taus		78	76.1	144	125.5
Many Jets + Taus		8	9.7	17	15.0

4 Interpretation within the MSSM framework

For all selections, the number of candidate events observed in the data is in agreement with the Standard Model background expectations. The results of the selections have been used to set limits on the MSSM parameter space.

The cross-section limits were evaluated at 208 GeV. Data taken at lower centre-of-mass energies also contribute to the limits with a reduced weight. The weight was calculated from the expected evolution of the cross section with \sqrt{s} .

The systematic uncertainties on the selection efficiencies are of the order of 4–5% and are dominated by the statistics of the simulated signal samples, with small additional contributions from lepton identification and energy flow simulation. They were taken into account by reducing the selection efficiencies by the estimated systematic uncertainty.

When setting the limits, background subtraction was performed for two- and four-fermion final states according to the prescription described in Ref. [18]. The systematic uncertainty on the expected Standard Model background has been evaluated by detailed comparison of the simulation with the data on control samples obtained with relaxed cuts. The subtracted background has been reduced by the systematic uncertainty derived from these comparisons (typically a few percent depending on the analysis). For the $We\nu$ and Zee processes the subtracted background has been further reduced by 20% due to the poor knowledge of the production cross section in the kinematic region selected by this analysis. No background is subtracted for the $\gamma\gamma \rightarrow f\bar{f}$ process.

The absolute lower limit on the mass of the lightest neutralino of 23 GeV/ c^2 obtained in Ref. [4] for a dominant $LL\bar{E}$ coupling, which is valid for any choice of μ , M_2 , m_0 (the unified sfermion mass term at the GUT scale) and generational indices (i , j and k), is used to restrict the range of neutralino mass considered for the indirect decays of the $LL\bar{E}$ searches.

The limits on sfermion masses derived from searches and indirect constraints obtained at LEP1 are discussed in Ref. [9]. They range from 40 to 45 GeV/ c^2 and are indicated on the exclusion plots.

4.1 Charginos and neutralinos decaying via $LL\bar{E}$

The results are interpreted assuming large scalar masses ($m_0 = 500$ GeV/ c^2). Depending on the masses of the gauginos and on the lepton flavour composition in the decay, the indirect decays of charginos to neutralinos populate different regions in track multiplicity, visible mass and leptonic energy. The “Leptons and Hadrons” selection, optimized for each possible topology, is used.

In the framework of the MSSM, 95% C.L. exclusion limits are derived in the (μ, M_2) plane as shown in Fig. 3a for $\tan\beta = 1.41$. The corresponding lower limit on the mass of the lightest chargino is 103 GeV/ c^2 .

The searches for the lightest and second lightest neutralino do not extend the excluded region in the (μ, M_2) plane beyond that achieved with the chargino search alone.

4.2 Squarks decaying via $LL\bar{E}$

Squarks cannot decay directly with an $LL\bar{E}$ coupling but they may decay indirectly via the lightest neutralino. Because the resulting topology is close to that arising from the indirect chargino decay, the “Leptons and Hadrons” selection is used. The 95% C.L. squark mass limits are presented as functions of m_χ in Fig. 4 for the case of \tilde{t}_1 and \tilde{b}_1 squarks. The results are displayed for left-handed squarks and for the values of the mixing angle for which the coupling to the Z vanishes. In the case of purely left-handed squarks, the following limits can be derived: $m_{\tilde{t}_L} > 91 \text{ GeV}/c^2$ and $m_{\tilde{b}_L} > 90 \text{ GeV}/c^2$ for any λ_{ijk} .

4.3 Sleptons decaying via $LL\bar{E}$

A slepton can decay directly via the $LL\bar{E}$ coupling to a lepton and anti-neutrino, hence the “Acoplanar Leptons” selection is used. For a given choice of $LL\bar{E}$ coupling, the decay of a right-handed slepton produces two different final states, $\tilde{\ell}_R^k \rightarrow \ell^i \bar{\nu}_{\ell^j}$ or $\bar{\nu}_{\ell^i} \ell^j$, with equal branching ratios. Excluded cross sections are shown in Fig. 5a for the different mixtures of acoplanar lepton states. The MSSM production cross sections for right-handed smuon pairs, and for selectron pairs at $\mu = -200 \text{ GeV}/c^2$ and $\tan \beta = 2$, are superimposed. The cross section limits translate into lower bounds of $m_{\tilde{\mu}_R, \tilde{\tau}_R} > 87 \text{ GeV}/c^2$ and $m_{\tilde{e}_R} > 96 \text{ GeV}/c^2$ ($\mu = -200 \text{ GeV}/c^2$, $\tan \beta = 2$).

Indirect decays of sleptons are selected using the “Six Leptons + \cancel{E} ” selection. Limits corresponding to this case are shown in Figs. 5b, 5c and 5d. Using the bound of $m_\chi > 23 \text{ GeV}/c^2$ these limits can be interpreted as the mass limits $m_{\tilde{e}_R} > 96 \text{ GeV}/c^2$ ($\mu = -200 \text{ GeV}/c^2$, $\tan \beta = 2$), $m_{\tilde{\mu}_R} > 96 \text{ GeV}/c^2$ and $m_{\tilde{\tau}_R} > 95 \text{ GeV}/c^2$.

4.4 Sneutrinos decaying via $LL\bar{E}$

Sneutrinos can decay directly via $LL\bar{E}$ into pairs of charged leptons. For pair produced sneutrinos, the final states, depending on the generation indices, are eeee, ee $\mu\mu$, ee $\tau\tau$, $\mu\mu\mu\mu$, $\mu\mu\tau\tau$ and $\tau\tau\tau\tau$, and can be selected with the “Four Lepton” selection. The exclusion limits on the sneutrino pair production cross section are shown in Fig. 6a. These limits translate into a lower bound on the electron sneutrino mass of $m_{\tilde{\nu}_e} > 100 \text{ GeV}/c^2$ ($\mu = -200 \text{ GeV}/c^2$, $\tan \beta = 2$) and the muon sneutrino mass of $m_{\tilde{\nu}_\mu} > 90 \text{ GeV}/c^2$.

Indirect decays of sneutrinos are selected using the “Four Leptons + \cancel{E} ” selection. The limits in the $(m_\chi, m_{\tilde{\nu}})$ plane corresponding to this case are shown in Figs. 6b and 6c. Using the bound $m_\chi > 23 \text{ GeV}/c^2$ this limit can be interpreted as $m_{\tilde{\nu}_{\mu,\tau}} > 89 \text{ GeV}/c^2$ and $m_{\tilde{\nu}_e} > 98 \text{ GeV}/c^2$, where the cross section for the electron sneutrino is evaluated at $\mu = -200 \text{ GeV}/c^2$ and $\tan \beta = 2$.

4.5 Charginos and neutralinos decaying via $LQ\bar{D}$

The results are interpreted assuming large scalar masses ($m_0 = 500 \text{ GeV}/c^2$). For the various topologies produced in the indirect decays of the chargino pairs via an $LQ\bar{D}$ coupling, the “MultiJets + Leptons” selection is used.

In the framework of the MSSM, 95% C.L. exclusion limits are derived in the (μ, M_2) plane as shown in Fig. 3b. The corresponding lower limit on the mass of the lightest chargino is $103 \text{ GeV}/c^2$.

The searches for the lightest and second lightest neutralino do not extend the excluded region in the (μ, M_2) plane beyond that achieved with the chargino search alone.

4.6 Squarks decaying via $LQ\bar{D}$

A squark can decay directly via $LQ\bar{D}$ to a quark and either a lepton or a neutrino, leading to topologies with acoplanar jets and up to two leptons. Couplings with electrons or muons in the final state are not considered as existing limits from the Tevatron [19] exclude the possibility of seeing such a signal at LEP. To select $\tilde{q} \rightarrow q\tau$ and $\tilde{q} \rightarrow q\nu$, the “2J+2 τ ” and the “AJ-H” selections are used. Examples of limits for squark production are shown in Fig. 7. In particular, for a dominant λ'_{33k} coupling, which implies $\text{Br}(\tilde{t}_L \rightarrow q\tau) = 100\%$, a lower limit of $m_{\tilde{t}_L} > 97 \text{ GeV}/c^2$ is obtained.

Indirect decays of squarks via the $LQ\bar{D}$ operator lead to six jets and up to two charged leptons. The selections used are “Jets-HM”, “4 Jets + 2 τ ”, “5 Jets + 1 Iso. ℓ ” and “Multi-jets plus Leptons”.

Limits for left-handed squarks are shown in Fig. 8. The following limits for \tilde{t}_L and \tilde{b}_L are derived: $m_{\tilde{t}_L} > 85 \text{ GeV}/c^2$ and $m_{\tilde{b}_L} > 80 \text{ GeV}/c^2$.

4.7 Sleptons and Sneutrinos decaying via $LQ\bar{D}$

Direct decays of sleptons and sneutrinos via the $LQ\bar{D}$ operator lead to four-jet final states. The “Four-Jets” selection is applied. The distributions of the di-jet masses for data and Monte Carlo are shown in Figs. 9a and 9b. Limits are derived by sliding a mass window of $5 \text{ GeV}/c^2$ across the di-jet mass distribution. The results are shown in Fig. 9c and imply $m_{\tilde{\nu}_\mu} > 79 \text{ GeV}/c^2$ and $m_{\tilde{\mu}_L} > 81 \text{ GeV}/c^2$.

Indirect decays of the sleptons via the $LQ\bar{D}$ operator yield two, three or four leptons and four jets in the final state; two leptons are of the same flavour as the initial sleptons. The indirect decays of sneutrinos produce a final state with four jets, up to two leptons and missing energy. For selectrons and smuons the “4 Jets + 2 Iso. ℓ ” selection is used except for the special case of $\lambda'_{3jk} \neq 0$ and $(m_{\tilde{t}_R} - m_\chi) < 10 \text{ GeV}/c^2$ where the “4 Jets + 2 τ ” selection is used. Indirect stau decays are selected with the “5 Jets + 1 Iso. ℓ ” selection if $m_\chi > 20 \text{ GeV}/c^2$ and either $\lambda'_{2jk} \neq 0$ or $\lambda'_{1jk} \neq 0$. The combination of the “5 Jets + 1 Iso. ℓ ”

and the “Leptons and Hadrons” selections is used otherwise. The sneutrinos are selected with the “4JH” selection for $m_\chi > 20 \text{ GeV}/c^2$ and “AJ-H” (acoplanar jets) otherwise. Limits for sleptons with indirect decays are shown in Figs. 10 and 11 with the selectron and electron sneutrino cross sections evaluated at $\mu = -200 \text{ GeV}/c^2$ and $\tan\beta = 2$. The limits are $m_{\tilde{e}_R} > 93 \text{ GeV}/c^2$, $m_{\tilde{\mu}_R} > 90 \text{ GeV}/c^2$, $m_{\tilde{\tau}_R} > 76 \text{ GeV}/c^2$, $m_{\tilde{\nu}_e} > 91 \text{ GeV}/c^2$ and $m_{\tilde{\nu}_\mu} > 78 \text{ GeV}/c^2$.

4.8 Charginos and neutralinos decaying via $\bar{U}\bar{D}\bar{D}$

The decay of the lightest neutralino leads to six hadronic jets in the final state. The indirect decays of a chargino or the second lightest neutralino give rise to a variety of final states which range from ten hadronic jets to six jets associated with leptons and missing energy. The “Many Jets”, “Four Jets” and “Many Jets + Lepton” selections are used to cover these topologies.

In the framework of the MSSM, 95% C.L. exclusion limits in the (μ, M_2) plane are obtained as shown in Fig. 3c. The lower limit on the lightest chargino mass is $103 \text{ GeV}/c^2$.

The searches for the lightest and second lightest neutralino do not extend the excluded region in the (μ, M_2) plane beyond that achieved with the chargino search alone.

4.9 Squarks decaying via $\bar{U}\bar{D}\bar{D}$

The direct decay of pair produced squarks leads to four-quark final states. The “Four Jet” selection is therefore used to extract the mass limits. As shown in Fig. 9c the mass limits are $82.5 \text{ GeV}/c^2$ for up-type squarks and $77 \text{ GeV}/c^2$ for down-type squarks.

For indirect squark decays, which lead to eight-jet topologies, the “Four Jets Broad” and “Four Jets” selections are used. Figure 12 shows the 95% C.L. exclusion limits in the $(m_\chi, m_{\tilde{q}})$ plane for left-handed stop and sbottom. The corresponding mass limits are $m_{\tilde{t}_L} > 71.5 \text{ GeV}/c^2$ and $m_{\tilde{b}_L} > 71.5 \text{ GeV}/c^2$.

4.10 Sleptons decaying via $\bar{U}\bar{D}\bar{D}$

No direct slepton decays are possible via the $\bar{U}\bar{D}\bar{D}$ coupling. For the indirect decays of pair produced selectrons and smuons, which lead to six-jet plus two-lepton final states, the “Four Jets + 2 Leptons” selection is used for large mass differences between the slepton and neutralino, and the “Many Jets + 2 Leptons” for the low mass difference region. In addition, for the very low mass difference region the leptons are very soft and the “Four Jets” selection is used. For indirect stau decays, which lead to six-jet plus two tau final states, the “Four Jets + Taus” and “Many Jets + Taus” selections are used for large and low mass differences between the stau and the neutralino, respectively.

The resulting 95% C.L. exclusion limits in the $(m_\chi, m_{\tilde{\ell}})$ plane are shown in Fig. 13. The selectron cross section is evaluated at $\mu = -200 \text{ GeV}/c^2$ and $\tan\beta = 2$. For $m_{\tilde{\ell}} - m_\chi > 10 \text{ GeV}/c^2$ this yields $m_{\tilde{e}_R} > 94 \text{ GeV}/c^2$, $m_{\tilde{\mu}_R} > 85 \text{ GeV}/c^2$ and $m_{\tilde{\tau}_R} > 70 \text{ GeV}/c^2$.

4.11 Sneutrinos decaying via $\bar{U}\bar{D}\bar{D}$

No direct sneutrino decays are possible via the $\bar{U}\bar{D}\bar{D}$ coupling. Sneutrinos decaying indirectly lead to six-jet final states plus two neutrinos. For small mass differences between the sneutrino and neutralino, the six jets are well separated and the ‘‘Many Jets + \cancel{E} ’’ selection is used. For large mass differences the event is characterized by a significant missing energy, and the ‘‘Four Jets + \cancel{E} ’’ selection is used.

The 95% C.L. exclusions in the $(m_\chi, m_{\tilde{\nu}})$ plane are shown in Fig. 14a for the electron sneutrino and in Fig. 14b for the muon or tau sneutrino. The electron sneutrino cross section is evaluated at $\mu = -200 \text{ GeV}/c^2$ and $\tan\beta = 2$. The limits $m_{\tilde{\nu}_e} > 88 \text{ GeV}/c^2$ and $m_{\tilde{\nu}_{\mu,\tau}} > 65 \text{ GeV}/c^2$ are obtained for $m_{\tilde{\nu}} - m_\chi > 10 \text{ GeV}/c^2$.

5 Summary

Pair production of supersymmetric particles, followed by direct or indirect decays involving R-parity violating couplings, has been searched for in the data collected with the ALEPH detector at LEP at centre-of-mass energies between 189 and 209 GeV. It has been assumed that the LSP has a negligible lifetime, and that only one λ_{ijk} , λ'_{ijk} or λ''_{ijk} coupling is nonzero. Several selections covering all the possible final states have been applied. No evidence for a signal has been found and various limits have been set within the framework of the MSSM with R-parity violating couplings. These results improve on those previously published by ALEPH [15] and by the other LEP collaborations [20].

The limits obtained for direct decays of sfermions are

- for an $LL\bar{E}$ coupling:
 - $m_{\tilde{e}_R} > 96 \text{ GeV}/c^2$ ($\mu = -200 \text{ GeV}/c^2$, $\tan\beta = 2$),
 - $m_{\tilde{\nu}_e} > 100 \text{ GeV}/c^2$ ($\mu = -200 \text{ GeV}/c^2$, $\tan\beta = 2$),
 - $m_{\tilde{\mu}_R, \tilde{\tau}_R} > 87 \text{ GeV}/c^2$,
 - $m_{\tilde{\nu}_\mu} > 90 \text{ GeV}/c^2$.
- for an $LQ\bar{D}$ coupling:
 - $m_{\tilde{\mu}_L} > 81 \text{ GeV}/c^2$,
 - $m_{\tilde{\nu}_\mu} > 79 \text{ GeV}/c^2$,
 - $m_{\tilde{t}_L} > 97 \text{ GeV}/c^2$ for $\text{Br}(\tilde{t}_L \rightarrow q\tau) = 1$.

- for a $\bar{U}\bar{D}\bar{D}$ coupling:
 - $m_{\tilde{u}_L} > 82.5 \text{ GeV}/c^2$,
 - $m_{\tilde{d}_L} > 77.0 \text{ GeV}/c^2$.

Table 5: The 95% confidence level lower mass limits for indirect sparticle decays for each of the three R-parity violating couplings, assuming $m_{\tilde{\ell},\tilde{\nu}} - m_\chi > 10 \text{ GeV}/c^2$ for $\bar{U}\bar{D}\bar{D}$ and $\mu = -200 \text{ GeV}/c^2$ and $\tan\beta = 2$ for \tilde{e} and $\tilde{\nu}_e$.

Sparticle	Lower mass limit (GeV/c^2)		
	$LL\bar{E}$	$LQ\bar{D}$	$\bar{U}\bar{D}\bar{D}$
\tilde{t}_L	91	85	71.5
\tilde{b}_L	90	80	71.5
\tilde{e}_R	96	93	94
$\tilde{\mu}_R$	96	90	85
$\tilde{\tau}_R$	95	76	70
$\tilde{\nu}_e$	98	91	88
$\tilde{\nu}_{\mu,\tau}$	89	78	65

For the indirect decays of sfermions, mass limits are listed in Table 5. For large sfermion masses, an absolute limit of $103 \text{ GeV}/c^2$ has been set on the chargino mass, irrespective of the R-parity violating operator.

6 Acknowledgements

It is a pleasure to congratulate our colleagues from the accelerator divisions for the successful operation of LEP at high energy. We would like to express our gratitude to the engineers and support people at our home institutes without whose dedicated help this work would not have been possible. Those of us from non-member states wish to thank CERN for its hospitality and support.

References

- [1] For a review see for example H.P. Nilles, Phys. Rep. **110** (1984) 1; H.E. Haber and G.L. Kane, Phys. Rep. **117** (1985) 75.
- [2] G. Farrar and P. Fayet, Phys. Lett. **B 76** (1978) 575.

- [3] S. Weinberg, Phys. Rev. **D 26** (1982) 287; N. Sakai and T. Yanagida Nucl. Phys. **B 197** (1982) 83; S. Dimopoulos, S. Raby and F. Wilczek, Phys. Lett. **B 212** (1982) 133.
- [4] ALEPH Collaboration, “*Search for supersymmetry with a dominant R-Parity violating $LL\bar{E}$ coupling in e^+e^- collisions at centre-of-mass energies of 130 GeV to 172 GeV*”, Eur. Phys. J. **C 4** (1998) 433.
- [5] ALEPH Collaboration, “*Search for R-Parity Violating Production of Single Sneutrinos in e^+e^- Collisions at $\sqrt{s} = 189\text{-}209$ GeV*”, CERN-EP-2001-094, submitted to Eur. Phys. J. **C**.
- [6] ALEPH Collaboration, “*ALEPH: a detector for electron-positron annihilations at LEP*”, Nucl. Instrum. and Methods **A 294** (1990) 121.
- [7] ALEPH Collaboration, “*Performance of the ALEPH detector at LEP*”, Nucl. Instrum. and Methods **A 360** (1995) 481.
- [8] S. Katsanevas and P. Morawitz, “*SUSYGEN 2.2 – A Monte Carlo event generator for MSSM Sparticle production at e^+e^- Colliders*”, Comp. Phys. Commun. **(112)** (1998) 227.
- [9] ALEPH Collaboration “*Search for R-parity violating decays of supersymmetric particles in e^+e^- collisions at centre-of-mass energies near 183 GeV*”, Eur. Phys. J. **C13** (2000) 29.
- [10] T. Sjöstrand, Comp. Phys. Commun. **82** (1994) 74.
- [11] M. Skrzypek, S. Jadach, W. Placzek and Z. Wąs, Comp. Phys. Commun. **94** (1996) 216.
- [12] S. Jadach, W. Placzek and B.F.L. Ward, Phys. Lett. **B 390** (1997) 298.
- [13] S. Jadach and Z. Wąs, Comp. Phys. Commun. **36** (1985) 191.
- [14] J.A.M. Vermaseren in “*Proceedings of the IVth International Workshop on Gamma Gamma Interactions*”, Eds. G. Cochar and P. Kessler, Springer Verlag, 1980; ALEPH Collaboration, “*An experimental study of $\gamma\gamma \rightarrow$ hadrons at LEP*”, Phys. Lett. **B 313** (1993) 509.
- [15] ALEPH Collaboration, “*Search for R-Parity Violating Decays of Supersymmetric Particles in e^+e^- Collisions at Centre-of-Mass Energies from 189 GeV to 202 GeV*”, Eur. Phys. J. **C 19** (2001) 415.
- [16] ALEPH Collaboration, “*Search for supersymmetry with a dominant R-Parity violating $LQ\bar{D}$ coupling in e^+e^- collisions at centre-of-mass energies of 130 GeV to 172 GeV*”, Eur. Phys. J. **C 7** (1999) 383.
- [17] ALEPH Collaboration, “*Search for charginos and neutralinos in e^+e^- collisions at centre-of-mass energies near 183 GeV and constraints on the MSSM parameter space*”, Eur. Phys. J. **C 11** (1999) 193.

- [18] D.E. Groom *et al.*, Particle Data Group, Eur. Phys. J. **C 15** (2000) 1.
- [19] D0 Collaboration, “*Search for second generation leptoquark pairs in $p\bar{p}$ collisions at $\sqrt{s} = 1.8$ TeV*”, Phys. Rev. Lett. **84** (2000) 2088;
CDF Collaboration, “*Search for Second and Third Generation Leptoquarks Including Production via Technicolor Interactions in $p\bar{p}$ Collisions at $\sqrt{s} = 1.8$ TeV*”, Phys. Rev. Lett. **85** (2000) 85;
D0 Collaboration, “*Search for First-Generation Scalar and Vector Leptoquarks*”, Phys. Rev. Lett. **D 64** (2001) 092004;
CDF Collaboration, “*Search for first generation leptoquark pair production in $p\bar{p}$ collisions at $\sqrt{s} = 1.8$ TeV*”, Phys. Rev. Lett. **79** (1997) 4327.
- [20] DELPHI Collaboration, “*Search for SUSY with R-parity violating $LL\bar{E}$ couplings at $\sqrt{s} = 189$ GeV*”, Phys. Lett. **B 487** (2000) 36;
DELPHI Collaboration, “*Search for R-parity violation with a $\bar{U}\bar{D}\bar{D}$ coupling at $\sqrt{s} = 189$ GeV*”, Phys. Lett. **B 500** (2001) 22;
L3 Collaboration, “*Search for R-parity violating decays of supersymmetric particles in e^+e^- collisions at LEP*”, Phys. Lett. **B 524** (2002) 65;
OPAL Collaboration, “*Searches for R-Parity violating decays of Gauginos at 183 GeV at LEP*”, Eur. Phys. J. **C 11** (1999) 619;
OPAL Collaboration, “*Search for R-parity Violating Decays of Scalar Fermions at LEP*”, Eur. Phys. J. **C 12** (2000) 1;

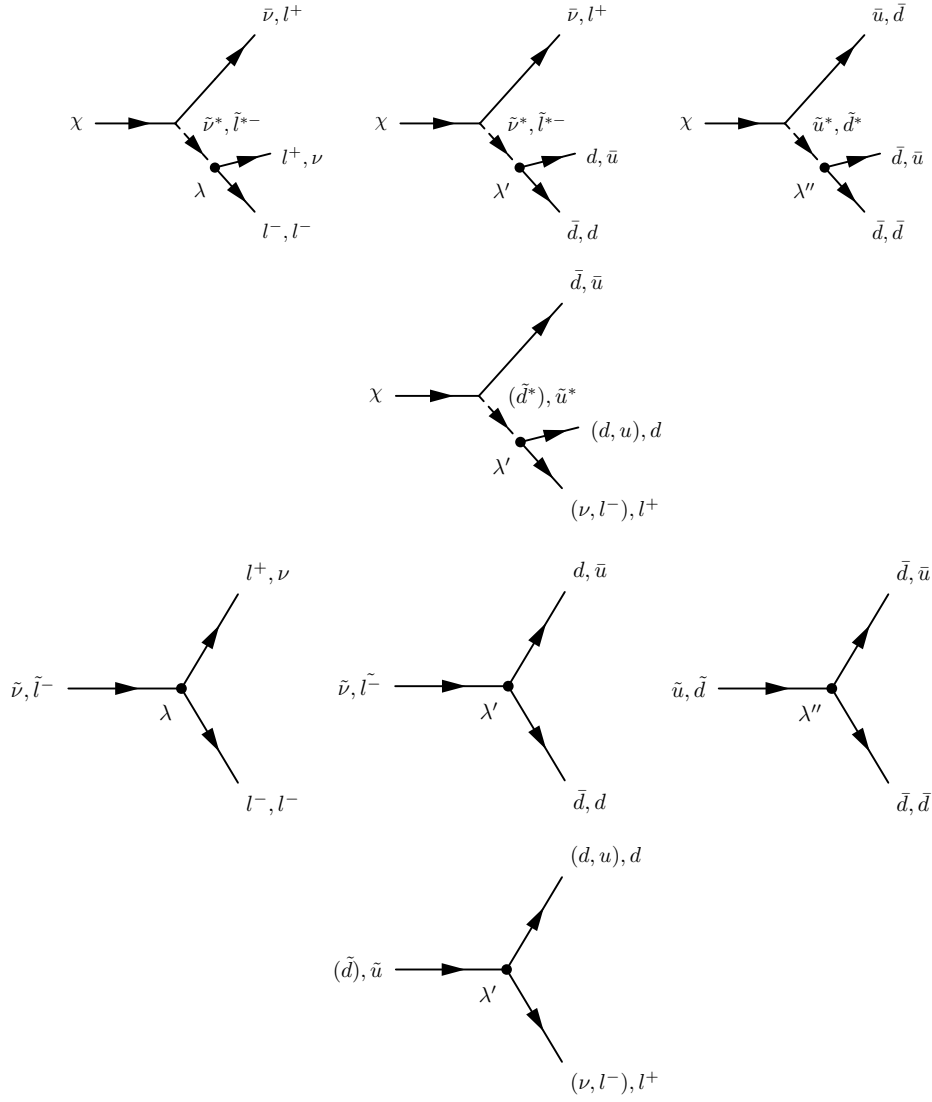


Figure 1: *Direct* R-parity violating decays of supersymmetric particles via the λ , λ' and λ'' couplings. The points mark the R-parity violating vertex in the decay.

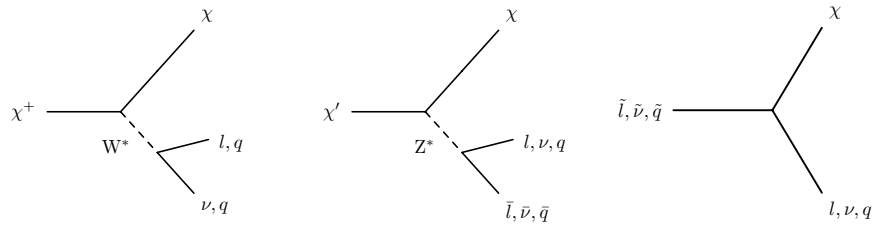


Figure 2: *Indirect* decays of supersymmetric particles. The neutralino χ decays directly via the λ , λ' and λ'' couplings as illustrated in Fig. 1.

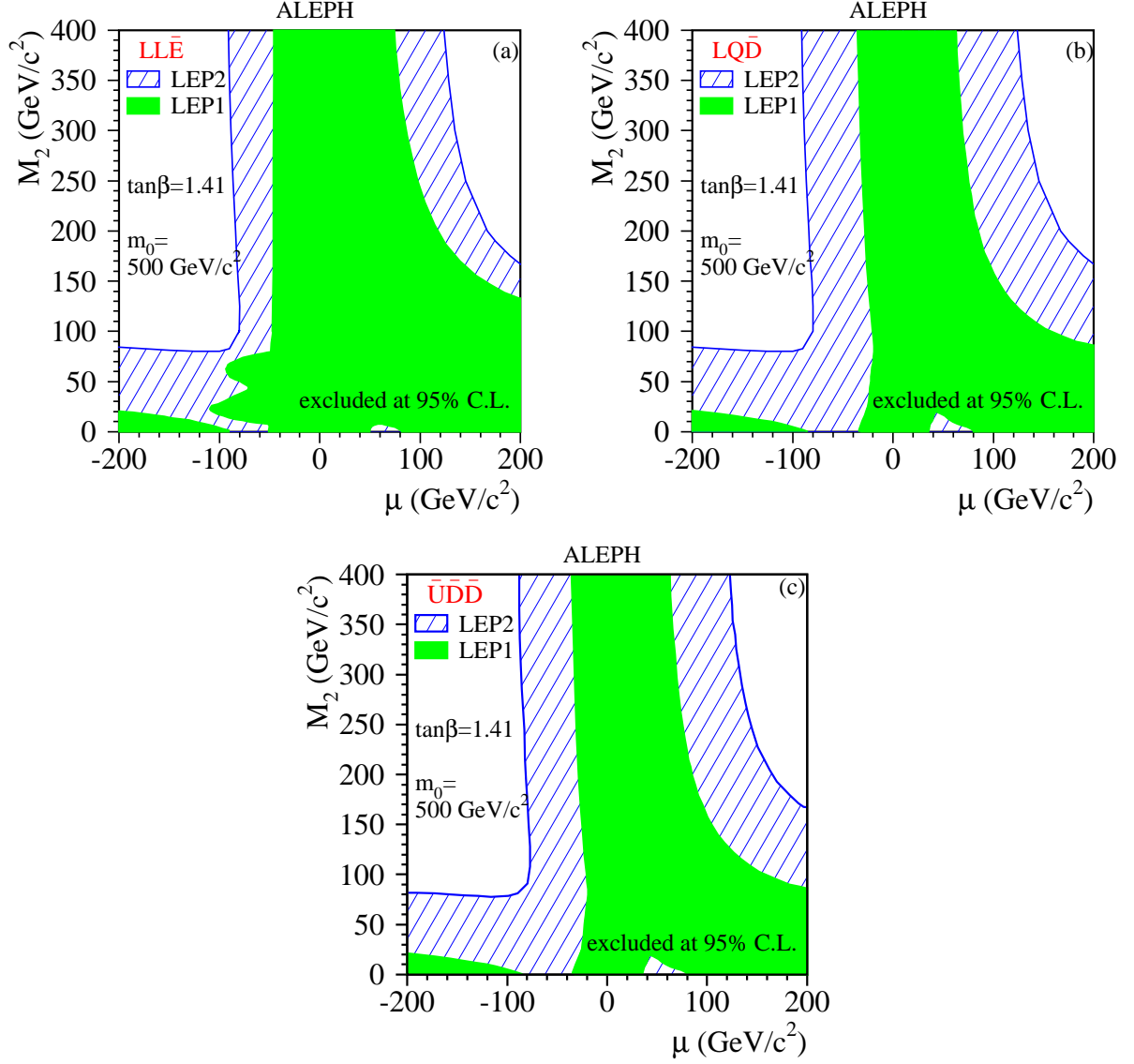


Figure 3: Regions in the (μ, M_2) plane excluded at 95% C.L. at $\tan\beta = 1.41$ and $m_0 = 500 \text{ GeV}/c^2$ for the three operators (a) λ , (b) λ' and (c) λ'' .

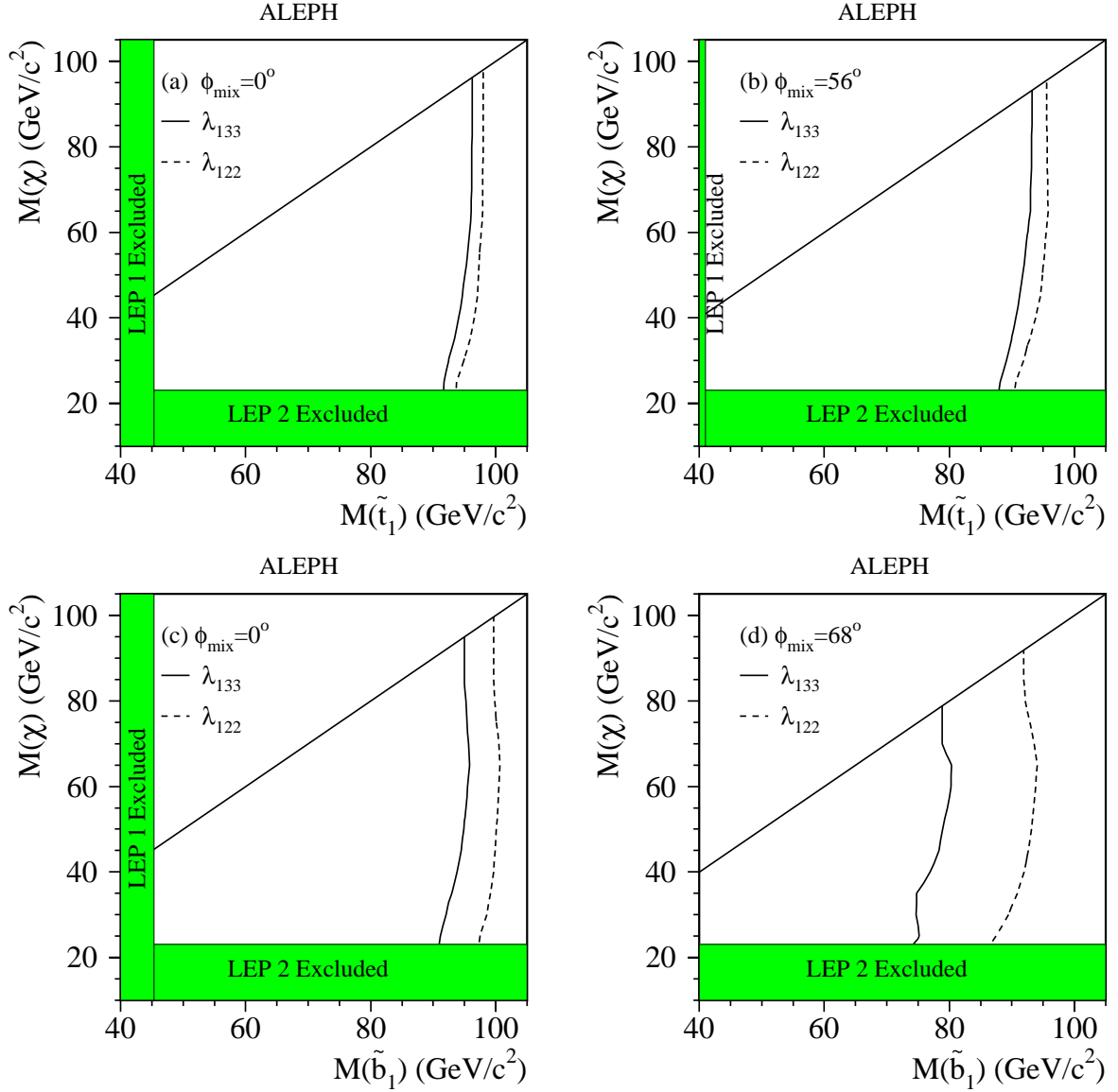


Figure 4: The 95% C.L. limits in (a),(b) the $(m_\chi, m_{\tilde{t}_1})$ plane and (c),(d) the $(m_\chi, m_{\tilde{b}_1})$ plane for indirect decays via the $LL\bar{E}$ couplings λ_{122} and λ_{133} , for no mixing ($\phi_{\text{mix}} = 0^\circ$) and for $\phi_{\text{mix}} = 56^\circ$ and 68° , corresponding to vanishing coupling to the Z, for stops and sbottoms, respectively. The LEP 2 exclusion corresponds to the absolute limit on m_χ .

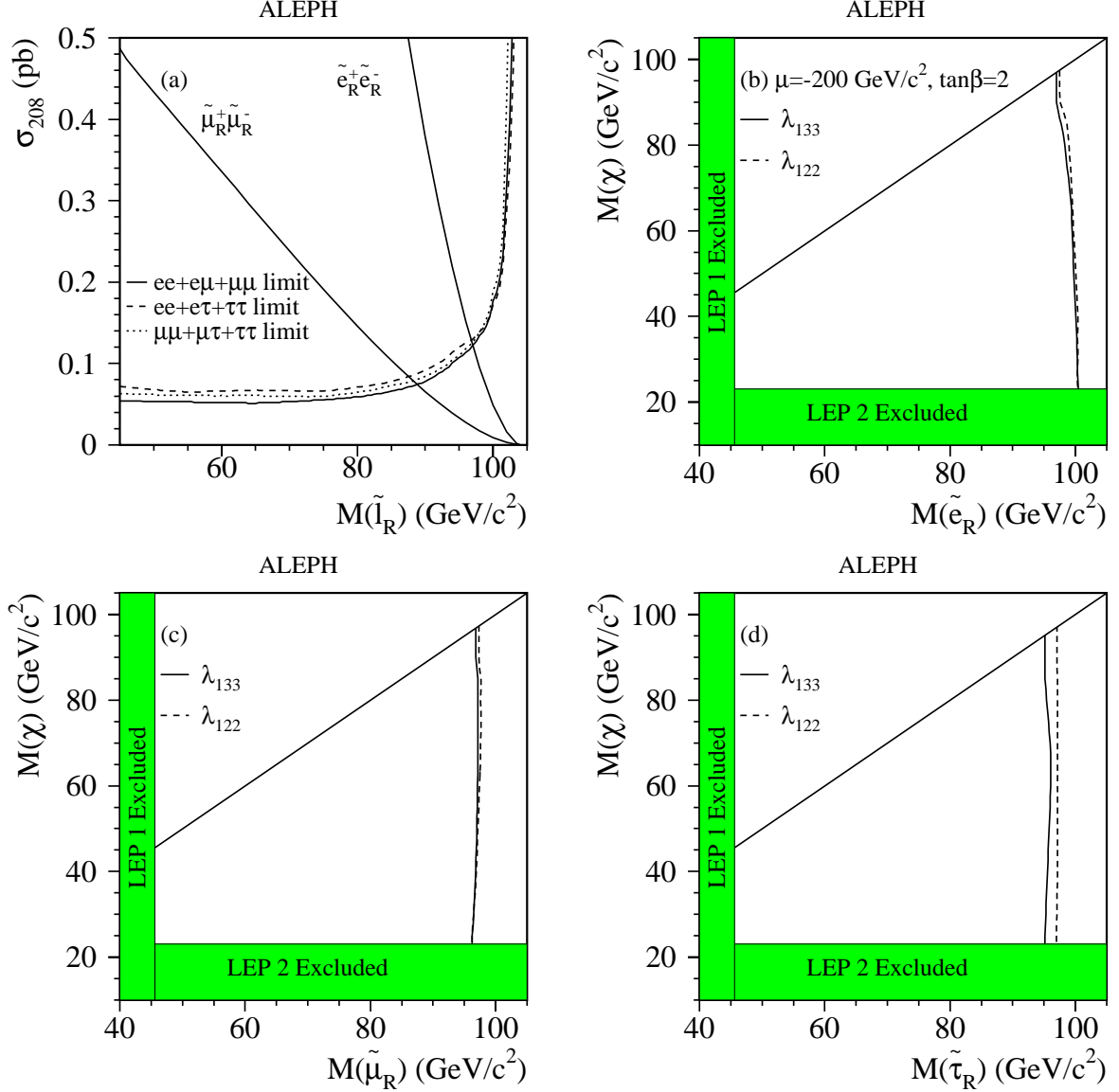


Figure 5: (a) The 95% C.L. cross-section upper limits for sleptons decaying directly via a dominant $LL\bar{E}$ operator. The MSSM cross sections for pair production of right-handed selectrons and smuons are superimposed. The 95% C.L. limits in the $(m_\chi, m_{\tilde{l}_R})$ plane for indirect decays of selectrons (b), smuons (c) and staus (d). The two choices of λ_{122} and λ_{133} correspond to the most and least stringent exclusions, respectively. The selectron cross section is evaluated at $\mu = -200 \text{ GeV}/c^2$ and $\tan\beta = 2$.

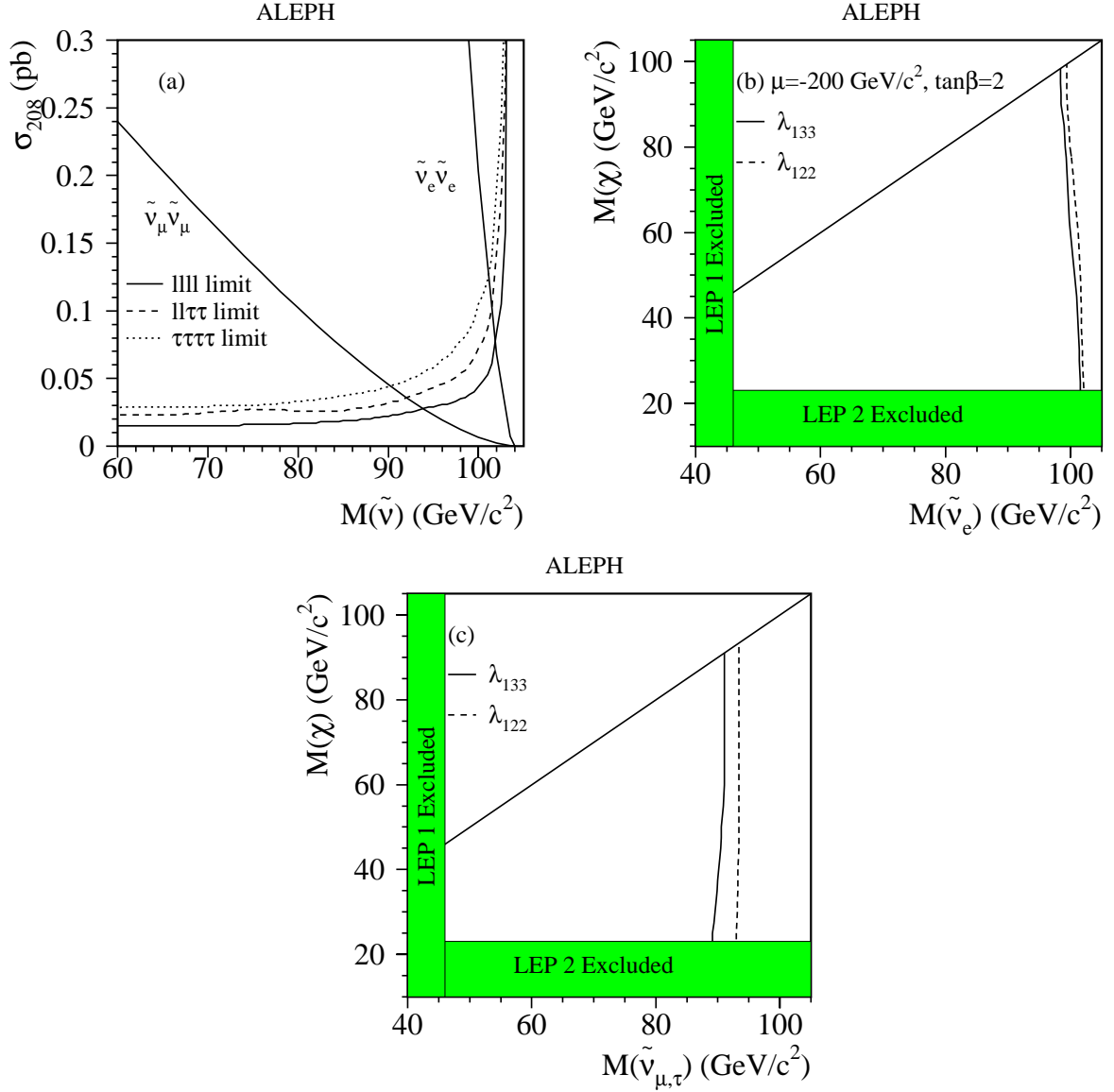


Figure 6: (a) The 95% C.L. cross-section upper limits for sneutrinos decaying directly via a dominant $LL\bar{E}$ operator. The three curves correspond to different possible final states, with $\ell = e$ or μ , due to the specific choice of sneutrino flavour and λ_{ijk} . The MSSM cross section for pair production of muon and electron sneutrinos are superimposed; the tau sneutrinos have the same cross section as the muon type. The 95% C.L. limits in the $(m_\chi, m_{\tilde{\nu}_e})$ plane for $\tilde{\nu}_e$ (b) and for both $\tilde{\nu}_\mu$ and $\tilde{\nu}_\tau$ (c) indirect decays. The two choices of λ_{122} and λ_{133} correspond to the most and least stringent exclusions, respectively. The electron sneutrino cross section is evaluated at $\mu = -200 \text{ GeV}/c^2$ and $\tan\beta = 2$.

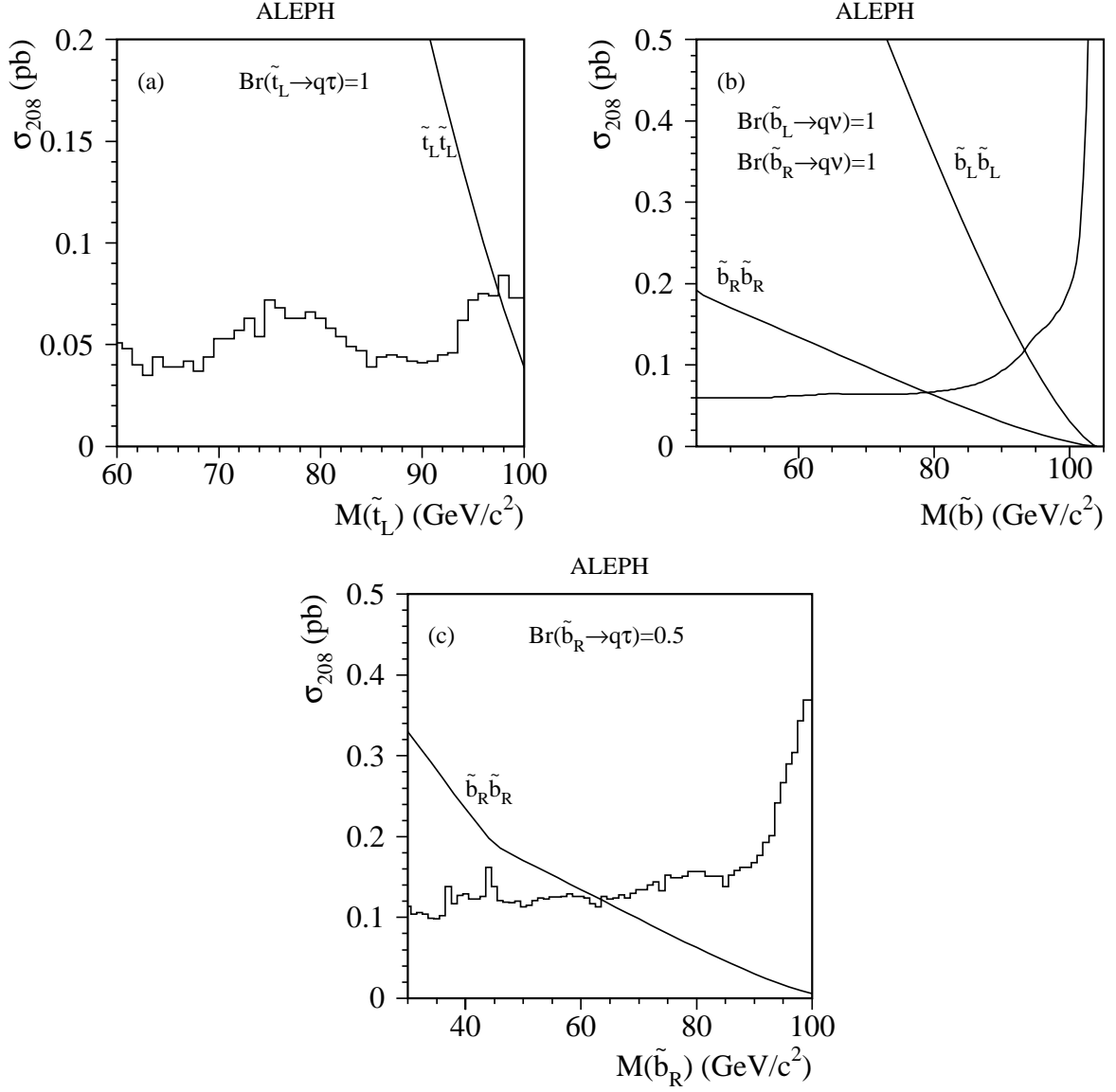


Figure 7: The 95% C.L. cross section upper limits for the production of squarks decaying directly via a dominant $LQ\bar{D}$ operator: the limits are shown for \tilde{t}_L (λ'_{33k}), \tilde{b}_L (λ'_{i3k}) or \tilde{b}_R (λ'_{i33}), and \tilde{b}_R (λ'_{3j3}) in (a), (b) and (c), respectively. The expected MSSM cross sections are superimposed.

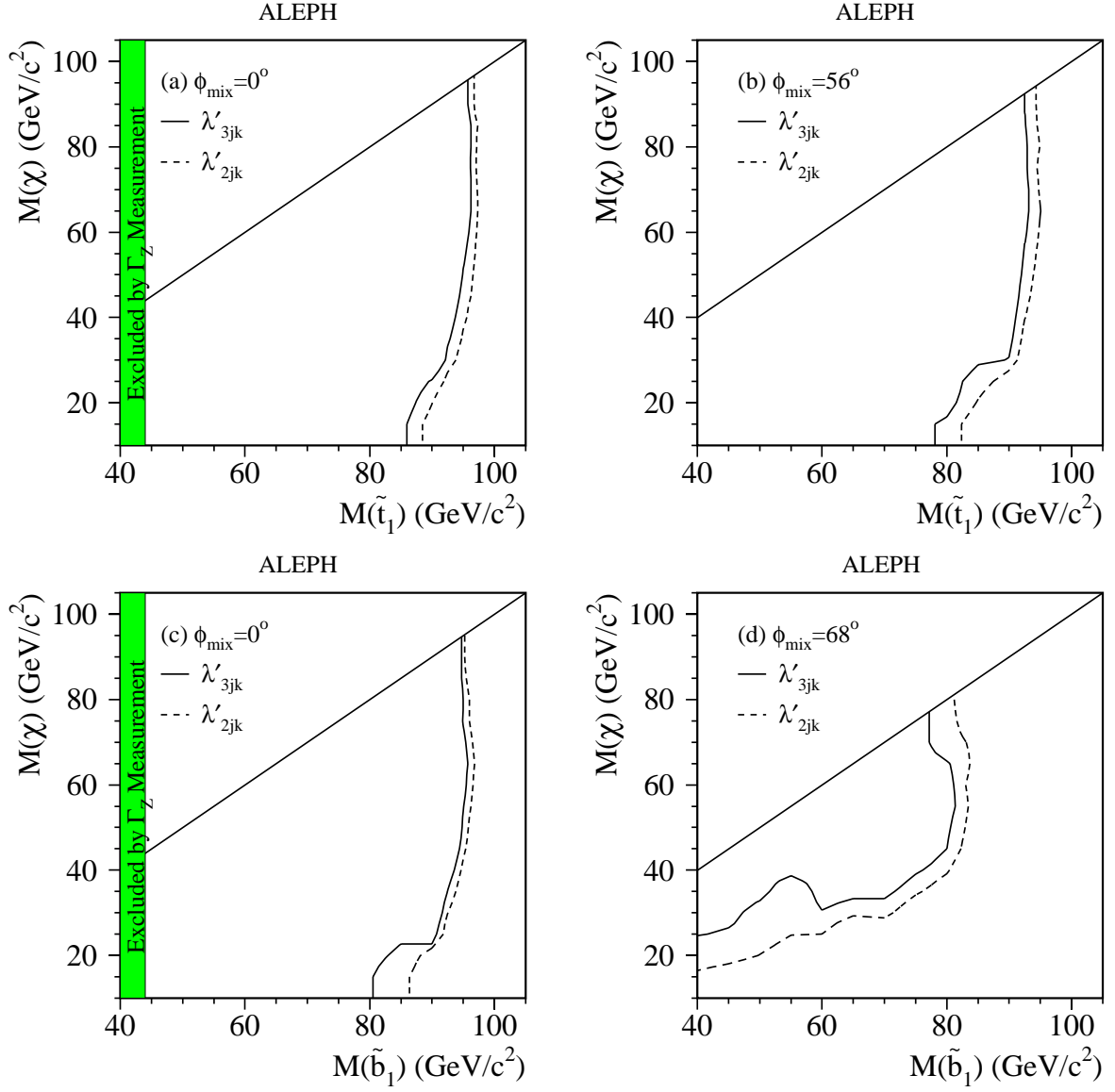


Figure 8: The 95% C.L. limits in (a),(b) the $(m_\chi, m_{\tilde{t}_1})$ plane and (c),(d) the $(m_\chi, m_{\tilde{b}_1})$ plane for indirect decays via a λ'_{211} or λ'_{311} $LQ\bar{D}$ coupling, for no mixing ($\phi_{\text{mix}} = 0^\circ$) and for $\phi_{\text{mix}} = 56^\circ$ and 68° for stops and sbottoms, respectively.

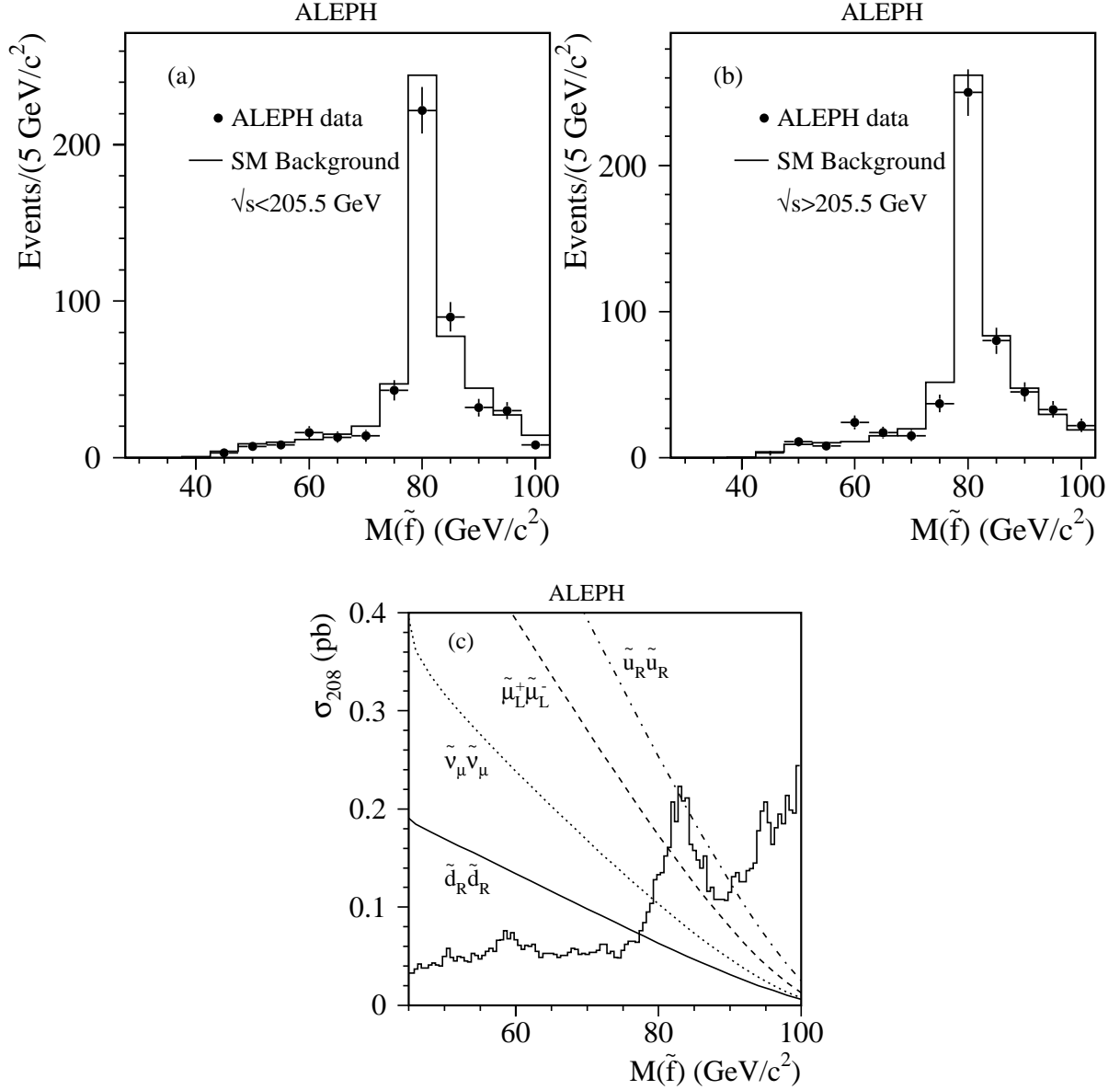


Figure 9: The distributions of the reconstructed jet-pair invariant masses after forcing each event into four jets. The points are the data taken in year 2000, for (a) the 205 GeV sample and for (b) the 207 GeV sample. The solid histogram is the predicted Standard Model background. In (c), the 95% C.L. cross section upper limit for sleptons (via $LQ\bar{D}$), sneutrinos (via $LQ\bar{D}$) and squarks (via $\bar{U}\bar{D}\bar{D}$) decaying directly to four jets is shown. The MSSM cross sections for pair production of muon sneutrinos, left-handed smuons and right-handed squarks are superimposed.

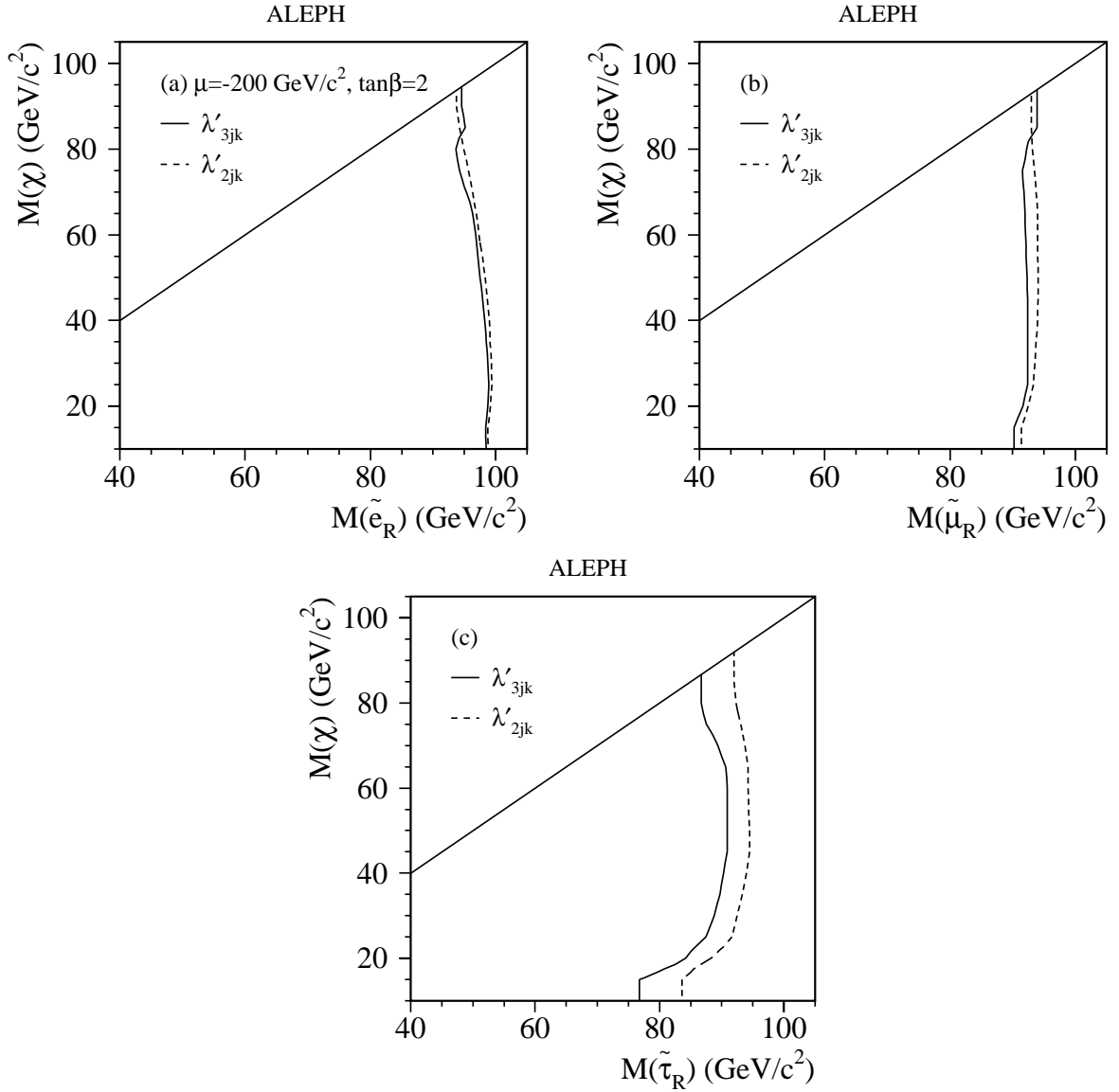


Figure 10: The 95% C.L. limits in the $(m_\chi, m_{\tilde{e}_R})$ plane for (a) selectrons, (b) smuons and (c) staus decaying indirectly via a dominant $LQ\bar{D}$ operator. The two choices of λ'_{2jk} and λ'_{3jk} correspond to the most and least stringent exclusions, respectively. The selectron cross section is evaluated at $\mu = -200 \text{ GeV}/c^2$ and $\tan\beta = 2$. The limit from the Γ_Z measurements excludes $m_{\tilde{e}} < 38 \text{ GeV}/c^2$.

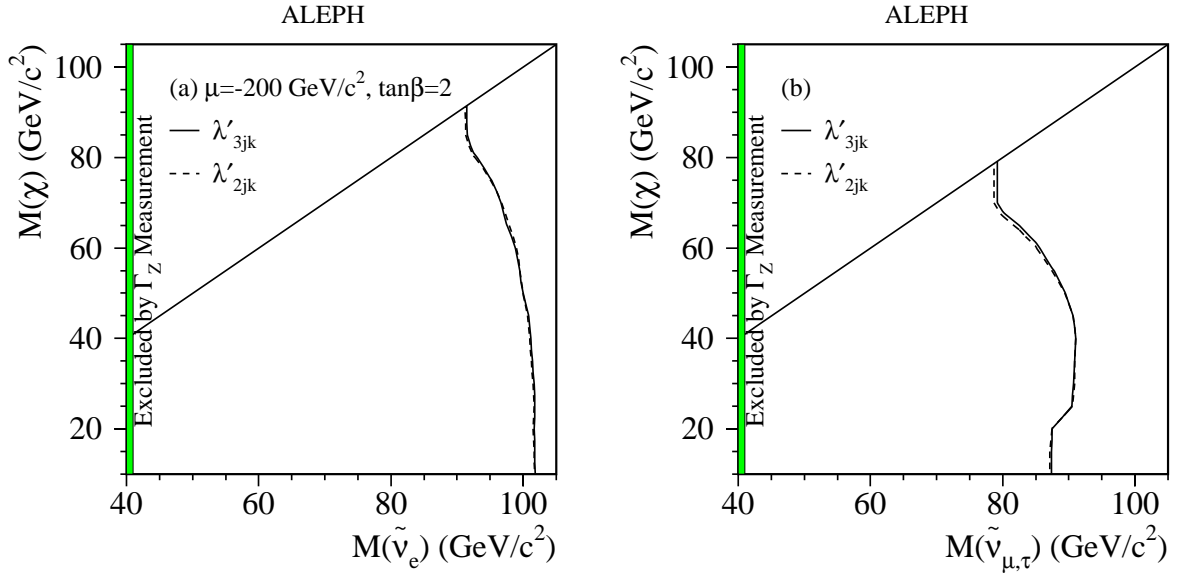


Figure 11: The 95% C.L. limits in the $(m_\chi, m_{\tilde{\nu}})$ plane for (a) electron and (b) muon or tau sneutrinos decaying indirectly via a dominant $LQ\bar{D}$ operator. The two choices of λ'_{2jk} and λ'_{3jk} correspond to the most and least stringent exclusions, respectively. The electron sneutrino cross section is evaluated at $\mu = -200 \text{ GeV}/c^2$ and $\tan\beta = 2$.

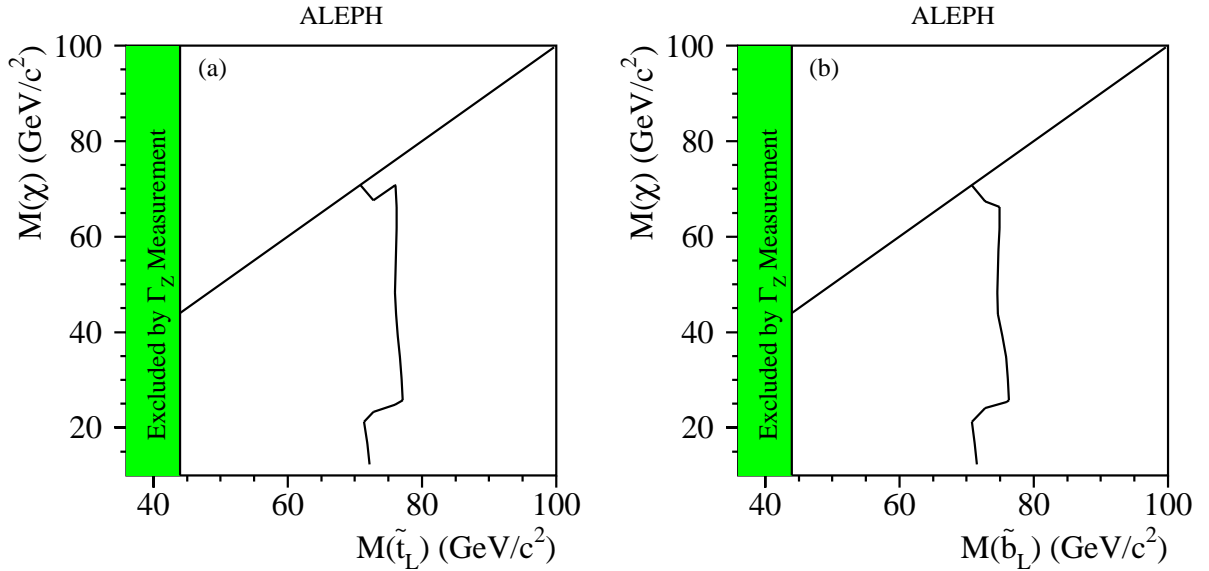


Figure 12: The 95% C.L. limits in (a) the $(m_\chi, m_{\tilde{t}_L})$ plane and (b) the $(m_\chi, m_{\tilde{b}_L})$ plane for indirect decays via the $\bar{U}\bar{D}\bar{D}$ couplings.

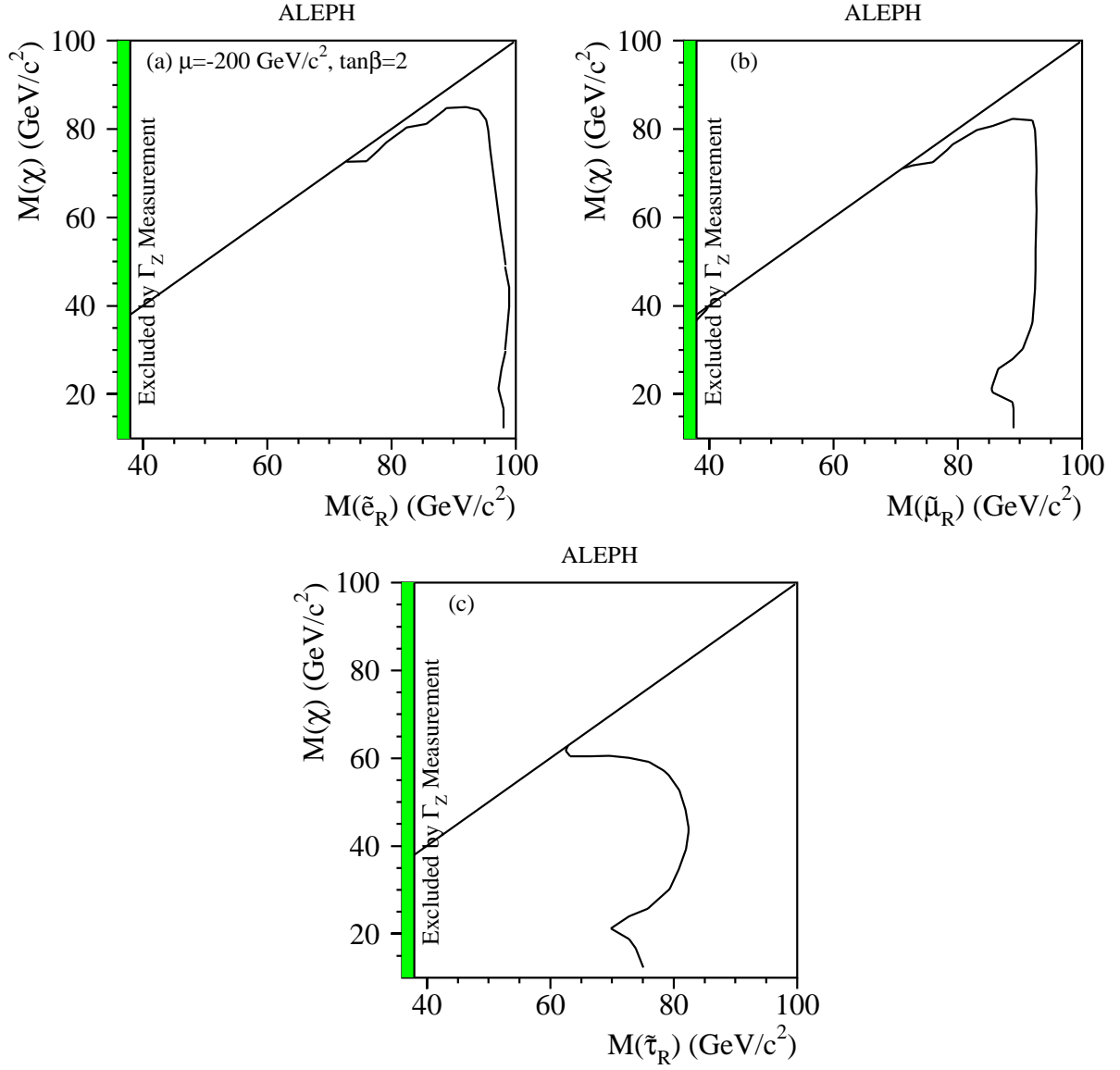


Figure 13: The 95% C.L. limits in the $(m_\chi, m_{\tilde{\ell}})$ plane for (a) selectrons, (b) smuons and (c) staus decaying indirectly via a dominant $\tilde{U}\tilde{D}\tilde{D}$ operator. The selectron cross section is evaluated at $\mu = -200 \text{ GeV}/c^2$ and $\tan\beta = 2$.

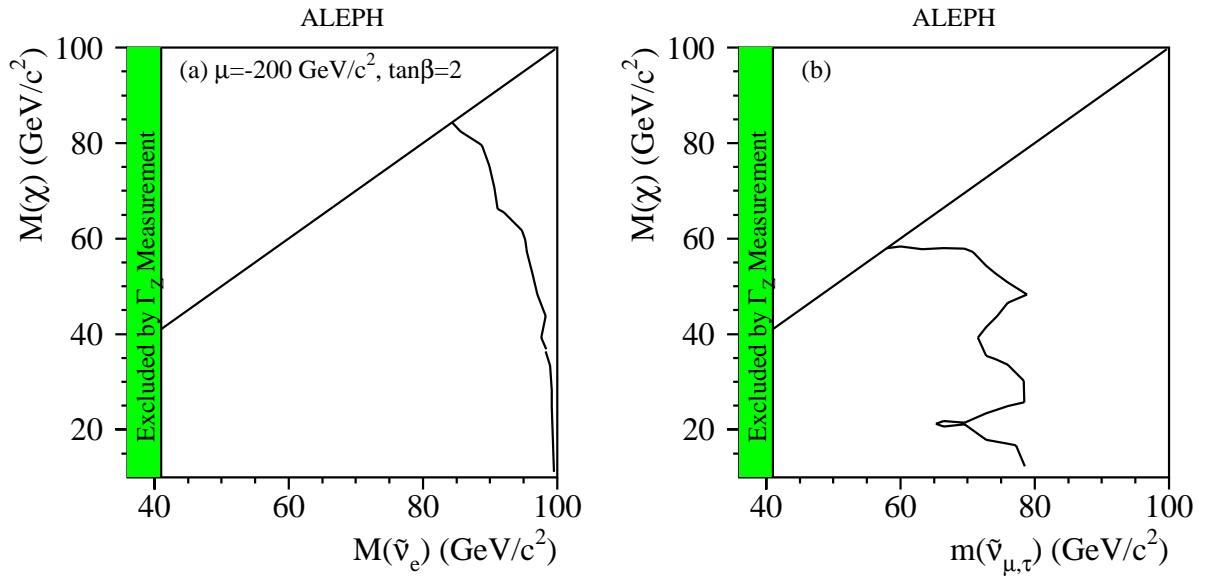


Figure 14: (a) The 95% C.L. limits in the $(m_\chi, m_{\tilde{\nu}})$ plane for $\tilde{\nu}_e$ decaying indirectly via a dominant $\bar{U}\bar{D}\bar{D}$ operator. The $\tilde{\nu}_e$ cross section is evaluated at $\mu = -200 \text{ GeV}/c^2$ and $\tan\beta = 2$. (b) The exclusion obtained in the $(m_\chi, m_{\tilde{\nu}_{\mu,\tau}})$ plane for $\tilde{\nu}_{\mu,\tau}$ decaying indirectly via a dominant $\bar{U}\bar{D}\bar{D}$ operator.